

Jiafeng Lu and Bin Ye

Abstract

Pre-shear history has been proven to be a critical factor in the liquefaction resistance of sand. In contrast to prior experimental studies in which triaxial shear tests were used to examine the effect of pre-shear on the liquefaction resistance of sand, hollow cylinder torsional shear tests were used in this study, to avoid the influence of inherent anisotropy that is inevitably produced during the sample preparation process due to gravitational deposition. A series of cyclic undrained shear tests were carried out on sand samples that had experienced different degrees of pre-shear loading. The test results showed that the liquefaction resistance of sand is greatly reduced by its pre-shear history, and a small pre-shear strain can cause sand to be much more prone to liquefaction. During the cyclic shear tests, the samples that had experienced pre-shear loading exhibited different behaviors when cyclic shear loading started in different directions, i.e. the clockwise direction and the counterclockwise direction.

Keywords

Pre-shear effect • Liquefaction • Hollow cylinder shear test • Anisotropy

15.1 Introduction

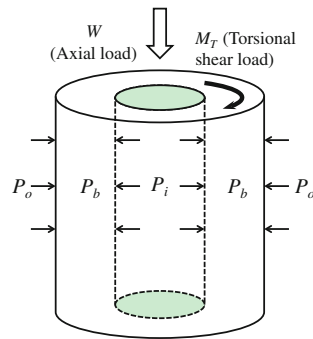
Liquefaction is a major threat to the safety of civil engineering structures constructed in sandy grounds when earthquakes occur. The liquefaction resistance of sand is governed by many factors, such as relative density, particle size gradation, particle shape etc. These normal factors have been studied extensively in the past few decades. In addition to these factors, the “pre-shear history” of sand is another factor that has a significant effect on its liquefaction resistance, but this factor has not received much attention. Finn et al. (1970) were the first researchers to note that the pre-shear history of sand can greatly influence its liquefaction resistance. Finn et al. (1970) demonstrated that a small pre-shearing can cause an increase in liquefaction resistance,

and a large pre-shearing can cause a drastic reduction in liquefaction resistance. Ishihara and Okata (1982) also found that the stress-induced anisotropy developed by pre-shearing can greatly influence the rate of increase of pore pressure during liquefaction. Recently, Yamada et al. (2010) and Ye et al. (2012) showed experimentally and theoretically that the pre-shearing induced by liquefaction can cause continuous, orderly and rapid changes in anisotropy, which influences the reliquefaction resistance of sand.

Most previous studies on the effect of pre-shear history on the liquefaction resistance of sand are based on experimental results obtained from triaxial shear tests. During triaxial compression or extension tests, stress-induced anisotropy develops in the same direction as the inherent anisotropy that is inevitably produced during the sample preparation process. However, this deficiency of the triaxial shear test apparatus can be overcome by another type of shear test, i.e., the hollow cylinder torsional shear test. In a hollow cylinder torsional shear test, the shear load can be applied along the horizontal plane, as shown in Fig. 15.1.

J. Lu · B. Ye (✉)
Tongji University, Siping Road 1239, Shanghai 200092, China
e-mail: yebinmail1977@gmail.com

Fig. 15.1 Torsional shear load applied to a hollow cylindrical sample



In this study, a series of hollow cylinder torsional shear tests were conducted to investigate how the liquefaction resistance of sand changes after pre-shear loading. The test results proved that pre-shearing can greatly reduce the liquefaction resistance of sand.

15.2 Description of the Hollow Cylinder Torsional Shear Test

The hollow cylinder testing apparatus can simultaneously impose axial load W , torque M_T , outer cell pressure P_o , inner cell pressure P_i and back pressure P_b (pore pressure) on the sample and control all five of them individually.

15.2.1 Sample Preparation

The tested sand in this study was Fujian standard sand, which is widely used in geotechnical experiments in China. The cumulative grain size distribution of the tested sand and physical properties are shown in Fig. 15.2 and Table 15.1, respectively.

The outer and inner diameters of the hollow cylindrical samples were 100 and 60 mm, respectively. The heights of the samples were 200 mm. Each sample was prepared by the water pluviation method. The Skempton's B value was

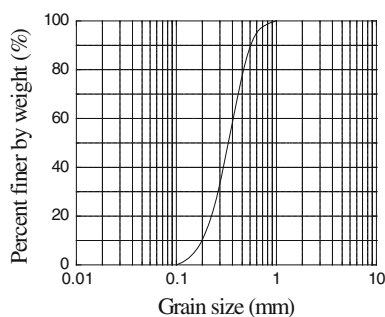


Fig. 15.2 Cumulative grain size distribution of the tested sand

Table 15.1 Physical properties of the tested sand

| | |
|---|------|
| Density of soil particles ρ_s (g/cm ³) | 2.64 |
| Maximum void ratio e_{\max} | 0.78 |
| Minimum void ratio e_{\min} | 0.50 |

0.96 or higher after the saturation procedure during which the mean effective stress was kept constant at 110 kPa.

15.2.2 Test Scheme

To investigate the pre-shear effect, the following test scheme was designed:

Stage 1: The samples were isotropically consolidated under equal outer and inner cell pressures of 200 kPa and a back pressure (pore pressure) of 90 kPa.

Stage 2: The consolidated samples were subjected to strain-controlled torsional shear loading under drained conditions. Table 15.2 lists the different degrees of pre-shear strain that were applied to the samples.

Stage 3: After the pre-shear strain reached the targeted value, the shear stress was unloaded to zero under drained conditions at the same rate that it was applied.

Stage 4: The samples were subjected to a cyclic torsional shear load under undrained conditions until liquefaction occurred.

The cyclic torsional loads were applied in sinusoidal mode, as shown in Fig. 15.3.

15.3 Test Results and Discussions

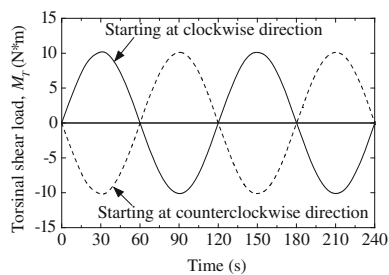
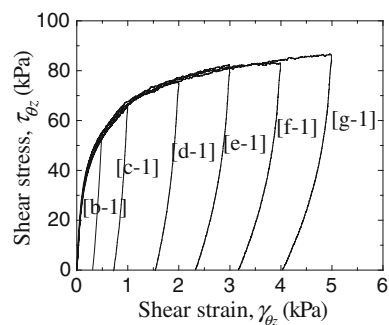
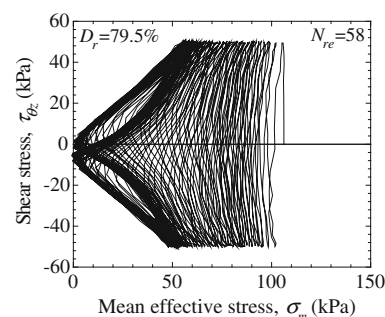
The stress–strain relations for Samples [b-1]–[g-1] in the pre-shear and subsequent unloading processes (Stages 2 and 3) are shown in Fig. 15.4. During the pre-shear tests, the mean effective stress of the sand was held constant under drained conditions. The changes in the relative densities of all samples were very small during the pre-shear tests.

15.3.1 Cyclic Shear Test on the Sample Without Pre-shear History

Figure 15.5 displays the stress path from the cyclic shear test of Sample [a], which had no pre-shear before cyclic shear loading. The parameter N_{re} , which is defined as the cycle number at which the mean effective stress of sand first reached the zero stress state, was used to indicate the liquefaction resistance of the sand.

Table 15.2 List of the tested samples

| Sample no. | Pre-shear strain, γ_{pr} (%) | D_r before pre-shear (%) | D_r after unloading (%) | Starting direction of cyclic shear load |
|------------|-------------------------------------|----------------------------|---------------------------|---|
| [a] | 0 | 79.5 | – | Clockwise |
| [b-1] | 0.5 | 79.5 | 80.0 | Clockwise |
| [b-2] | | | 79.8 | Counterclockwise |
| [c-1] | 1.0 | 79.5 | 79.9 | Clockwise |
| [c-2] | | | 79.8 | Counterclockwise |
| [d-1] | 2.0 | 79.5 | 79.8 | Clockwise |
| [d-2] | | | 79.8 | Counterclockwise |
| [e-1] | 3.0 | 79.5 | 79.5 | Clockwise |
| [e-2] | | | 79.7 | Counterclockwise |
| [f-1] | 4.0 | 79.5 | 78.3 | Clockwise |
| [f-2] | | | 79.0 | Counterclockwise |
| [g-1] | 5.0 | 79.5 | 78.5 | Clockwise |
| [g-2] | | | 78.2 | Counterclockwise |

**Fig. 15.3** Time history of the cyclic shear loads in the pre-shear tests**Fig. 15.4** Stress path and stress–strain relation**Fig. 15.5** Cyclic shear behavior of sample [a]

15.3.2 Cyclic Shear Tests on the Samples with Pre-shear History

Figure 15.6 displays the cyclic shear behaviors of Samples [b-1, 2]–[d-1, 2], which experienced pre-shear strains from 0.5 to 2 %. Comparing the stress paths in Figs. 15.5 and 15.6, it can be observed that the mean effective stresses of the samples with pre-shear history decreased much faster than that of Sample [a]. Many fewer loading cycles were required for Samples [c-1, 2], [d-1, 2] to reach the zero stress state.

From Fig. 15.6, it can also be observed that the shear tests begun in the clockwise direction and those begun in the counterclockwise direction resulted in almost the same values of N_{re} . However, the stress paths exhibit obvious differences, especially during the first half loading cycle. This difference can be theoretically explained by the development of stress-induced anisotropy, using rotational hardening theory (Zhang et al. 2007). During the pre-shear tests, the stress-induced anisotropy developed in the same direction as the pre-shear loading. The anisotropy can be represented by the upward rotation of the yield surface in the stress space, as shown in Figs. 15.7 and 15.8. After unloading, the anisotropy remained in the soil, and the yield surface still inclined upward. If the subsequent cyclic loading started in the clockwise direction (Fig. 15.7), the stress increment vector, $d\tau$, pointed toward the interior of the yield surface, and an unloading process began. Thus, the mean effective stress did not change under undrained conditions. Alternatively, if shear loading started in the counterclockwise direction (Fig. 15.8), the stress increment vector, $d\tau$, pointed outward from the yield surface, and the loading process started, causing the mean effective stress to decrease more substantially. In a more detailed comparison of the cyclic shear tests started in the clockwise and

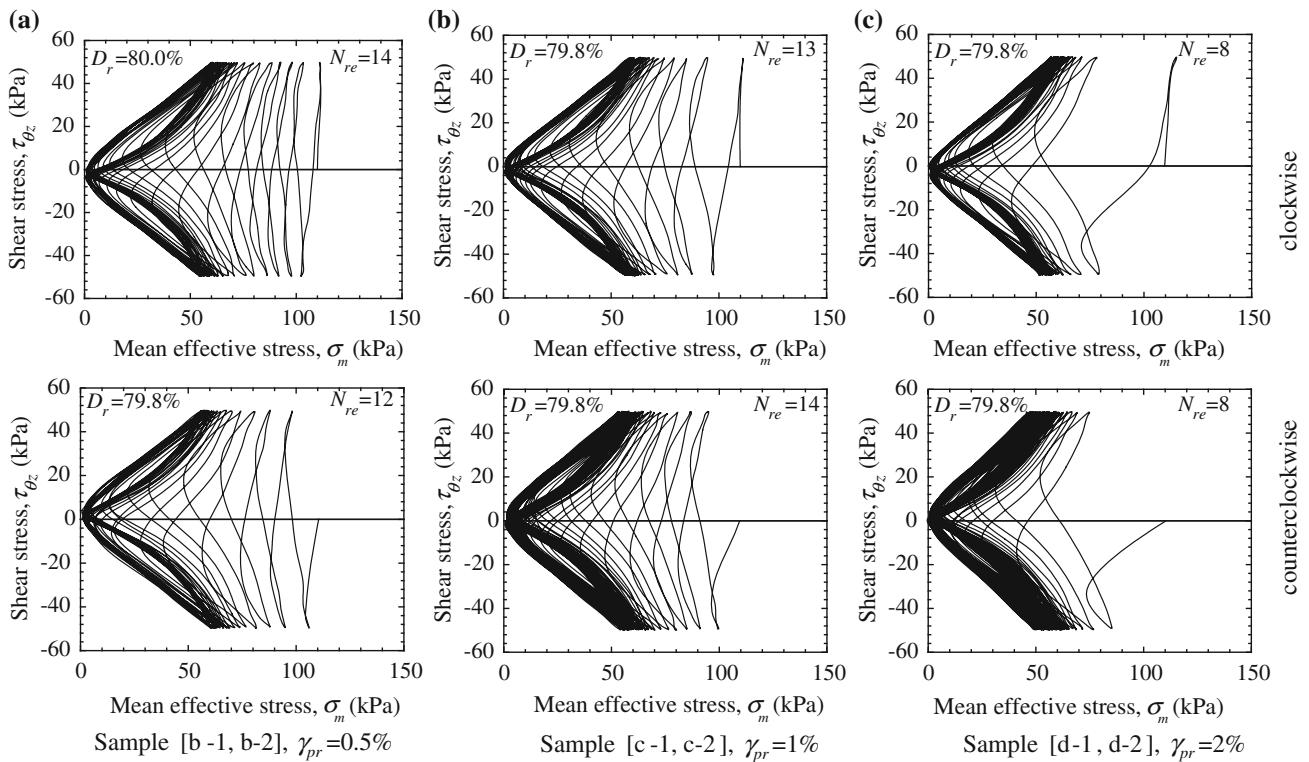


Fig. 15.6 Cyclic shear behavior of samples [b]–[h] (with pre-shear history)

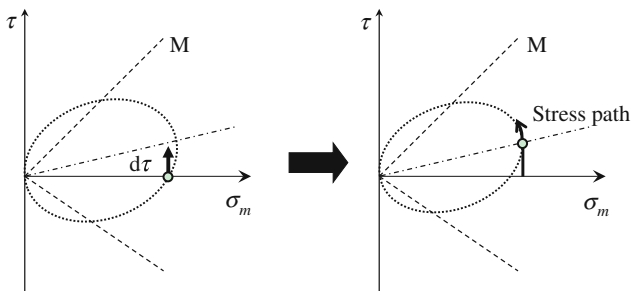


Fig. 15.7 Cyclic shear loading starting in the clockwise direction

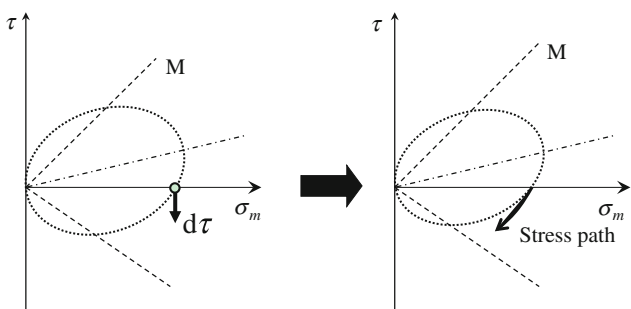


Fig. 15.8 Cyclic shear loading starting in the counterclockwise direction

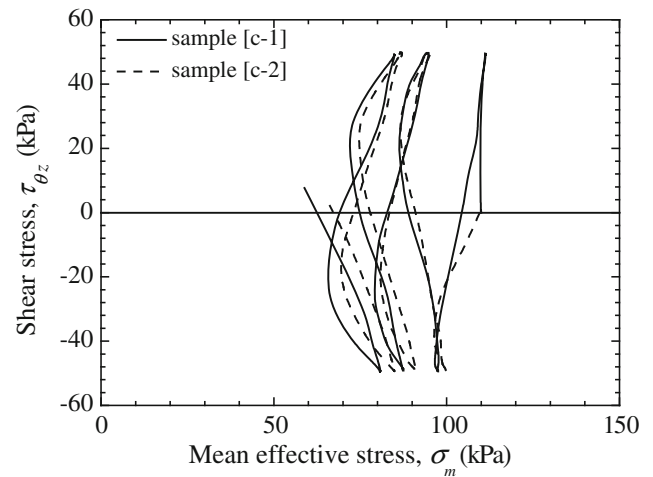


Fig. 15.9 Stress path of the first three cycles of cyclic loading of Samples [c-1] and [c-2]

counterclockwise directions, Fig. 15.9 illustrates the stress paths of Samples [c-1] and [c-2] during the first three loading cycles.

In addition, stress path of Sample [c-1] for the second half of the loading cycle was very similar to that of Sample [c-2] from the beginning. This implies that the anisotropic

state of Sample [c-1] after the first half of the loading cycle was close to the initial state of Sample [c-2]. This means that the influence of the anisotropy induced by pre-shearing nearly disappeared after the first loading cycle.

The above discussion suggests that the influence of pre-shear loading could lead to a substantial decrease in the liquefaction resistance of sand and that this influence runs through the whole liquefaction process.

15.4 Conclusions

In this study, hollow cylinder shear tests were carried out to examine the effect of pre-shear on the liquefaction resistance of sand. Cyclic undrained shear loadings were applied to samples that had experienced different degrees of pre-shear loading. The main conclusions drawn from the results of this study are summarized below.

- (1) The liquefaction resistance of sand is greatly influenced by its pre-shear history. Sand is more prone to liquefaction after experiencing pre-shear, even though its relative density is almost unchanged. The larger the pre-shear strain is, the lower the liquefaction resistance will be.
- (2) After pre-shear loading, sand exhibits anisotropic behavior during subsequent cyclic shear loading,

especially during the first loading cycle. From the second half of the loading cycle onward, the stress paths of the tests started in the clockwise direction were similar to those of the tests started in the counterclockwise direction.

- (3) The anisotropy induced by pre-shear loading disappeared after the first loading cycle. From the second loading cycle on, the anisotropy induced by the following cyclic loading played a more significant role in the liquefaction process.

References

- Finn WDL, Bransby PL, Pickering DJ (1970) Effects of strain history on liquefaction of sands. *Soil Mech Found Div Proc ASCE* 96(6):1917–1934
- Ishihara K, Okada S (1982) Effects of large preshearing on cyclic behavior of sand. *Soils Found* 22(3):109–125
- Yamada S, Takamori T, Sato K (2010) Effects on reliquefaction resistance produced by changes in anisotropy during liquefaction. *Soils Found* 50(1):9–25
- Ye B, GL Y, Zhang F (2012) Numerical modeling of changes in anisotropy during liquefaction using a generalized constitutive model. *Comput Geotech* 42:62–72
- Zhang F, Ye B, Noda T, Nakano M, Nakai K (2007) Explanation of cyclic mobility of soils: approach by stress-induced anisotropy. *Soils Found* 47(4):635–648